TẠP CHÍ KHOA HỌC
TRƯỜNG ĐẠI HỌC QUY NHƠN

Sử dụng mô hình tensor để mở rộng bài toán ước lượng kênh LS cho các hệ thống MIMO có hỗ trợ bề mặt phản xạ thông minh

Đào Minh Hưng*, Nguyễn Đỗ Dũng

Khoa Kỹ thuật và Công nghệ, Trường Đại học Quy Nhơn, Việt Nam

Ngày nhận bài: 25/07/2023; Ngày sửa bài: 06/09/2023;
Ngày nhận đăng: 18/09/2023; Ngày xuất bản: 28/10/2023

TÓM TẮT

Bài báo đề xuất mở rộng hai thuật toán ước lượng kênh LS dựa trên mô hình tín hiệu tensor cho các hệ thống MIMO được hỗ trợ bởi bề mặt phản xạ thông minh (IRS). Hai thuật toán này khai thác cấu trúc tensor của tín hiệu hoa tiêu để thiết lập bài toán ước lượng kênh ghép tầng. Thuật toán thứ nhất mở rộng ước lượng LS dựa trên việc khai thác cấu trúc Khatri-Rao Factorization (KRF) của kênh MIMO ghép tầng, bằng cách giải các bài toán con xấp xỉ ma trận hạng 1. Bài toán ước lượng thứ hai dựa trên thuật toán BALS (Bilinear Alternating Least Squares), đây là phiên bản đơn giản hóa của thuật toán TALS (Trilinear Alternating Least Squares). Ngoài ra, bài báo này cũng trình bày mối quan hệ giữa các tham số kênh MIMO để các thuật toán ước lượng trên có tính khả thi. Kết quả mô phỏng cho thấy các phương pháp ước lượng LS mở rộng dựa trên mô hình tín hiệu tensor đã cải thiện hiệu suất so với ước lượng LS truyền thống.

Từ khóa: *Ước lượng kênh, bề mặt phản xạ thông minh, thuật toán dựa trên tensor, Khatri-Rao factorization*.

**Tác giả liên hệ chính.*
Email: daominhhung@qnu.edu.vn

QUY NHON UNIVERSITY
JOURNAL OF SCIENCE

Using tensor model to extend least squares channel estimation problem for the intelligent reflecting surface assisted MIMO systems

Dao Minh Hung*, Nguyen Do Dung

Faculty of Engineering and Technology, Quy Nhon University, Vietnam

Received: 25/07/2023; Revised: 06/09/2023;
Accepted: 18/09/2023; Published: 28/10/2023

ABSTRACT

This paper proposes to extend two Least Squares (LS) channel estimation algorithms based on tensor signal model to MIMO systems supported by Intelligent Reflective Surfaces (IRS). These two algorithms exploit the tensor structure of the pilot signal to establish the cascaded channel estimation problem. The first algorithm extends the LS estimation based on exploiting the Khatri-Rao Factorization (KRF) structure of the cascaded MIMO channel, by solving subproblems approximating the 1-rank matrix. The second estimator is based on the Bilinear Alternating Least Squares (BALS) algorithm, which is a simplified version of the Trilinear Alternating Least Squares (TALS) algorithm. In addition, this paper also presents the relationship between the MIMO channel parameters for the above estimation algorithms to be feasible. The simulation results show that the extended LS estimation methods based on the tensor signal model have improved performance compared with the conventional LS estimation.

1. INTRODUCTION

Over the past decade, Multiple Input Multiple Output (MIMO) communication systems have been extensively studied and considered a key technology for enhanced mobile broadband communications in fifth generation networks (5G), the future beyond-5G (B5G) and sixth generation (6G). Several works have thoroughly investigated both theoretical and practical solutions on spectral efficiency analysis, data rate increase, reliability improvement and interference reduction, etc.[1-4] MIMO systems can be classified into different types, such as Single-User MIMO (SU-MIMO), Multi-User MIMO (MU-MIMO), massive MIMO and millimeter wave MIMO, depending on the number of user, the number of antennas and the operating frequency bands. MIMO systems can be applied in wireless communication systems, such as cellular networks, wireless Local Area Networks (WLANs), vehicle networks, satellite communications, and radar systems. Some trends in the application of MIMO systems include: Internet of Things (IoT) device systems, MIMO for Unmanned Aerial Vehicles (UAVs) and MIMO for cognitive radio networks.

The above mentioned advantages of MIMO systems are achieved by the outstanding

**Corresponding author.*
Email: daominhhung@qnu.edu.vn

https://doi.org/10.52111/qnjs.2023.17507

characteristic of channel hardening, i.e. the characteristic of user channels that do not fading over time and the favorable propagation over multipath channel. However, for MIMO systems, including massive MIMO, there is an open problem to ensure the performance of users in service dead zones, for example, indoor users with thick walls between them and the Base Station (BS) or outdoor users surrounded by many tall buildings, where gain is difficult to compensate for severe channel loss.

In the last few years, a number of studies have discussed the potentials and challenges of wireless communications assisted by Intelligent Reflective Surfaces (IRS).[5-7] Much research has been done on both the theory and implementation of IRS application in MIMO communication systems to maintain performance and increase user coverage in service dead zones. With the assistance of the IRS, MIMO systems can suppress Co-Channel Interference (CCI) when the user is at the edge of the cell,[8,9] or to improve physical layer security.[10,11] Besides, IRS can be used for information and power transfer in a IoT networks.[8] IRS also known as reconfigurable smart surface or software controlled hypersurface consisting of a 2D array with a large number of passive or semi-passive elements can control the electromagnetic characteristics of radio frequency waves so that the reflected signal adds coherently at the receiver or cancels it out to reduce CCI.[5-9] Each element can operate independently and can be reconfigured in a software-defined manner using an external controller. The IRS does not require dedicated Radio Frequency (RF) strings and is powered wirelessly by an external RF source. This is in contrast to relay systems that need amplify-and-forward or decode-and-forward, and require specialized power sources.[6]

In MIMO systems, the availability of Channel State Information (CSI) is a topic of intense research. Accurate and timely CSI knowledge plays an important role in wireless communication systems. For IRS-assisted MIMO systems, there are often a large number of IRS elements, which poses a significant challenge to solving the channel estimation problem in collecting CSI. In these systems, there are two basic methods for performing channel estimation. First, use the IRS with a semi-passive structure in which several active elements connected to receive the RF string. In this case, the parts that actively perform baseband processing at the IRS facilitate the collection of CSI.[12]

In the second method, the IRS has a full passive structure, where the IRS works by reflecting the impinging waves according some phase shift pattern. This is a more difficult case, where at the receiver based on the pilot signals sent by the transmitter and reflected by the IRS performs a cascade estimation between the transmitter to the IRS and the IRS to the receiver. In this case, the IRS uses a phase shift model in which the training phases play an important role. This is the method used in this paper.

A number of published works refer to different solutions to the channel estimation problem for the case of passive IRS. T. L. Jensen et al. have proposed an unbiased estimation method with minimal variance and an optimal calculation of the IRS phase shift matrix, in which the IRS elements are completely passive.[13] The authors in the reference,[14] propose a two-stage algorithm by exploiting the sparse code characteristics of multipath channels with low rank channel matrices. The cooperative channel estimation through the training beam of IRS-assisted massive MIMO systems on the terahertz channel is presented[15]. IRS was proposed as a solution to reduce the congestion problem and also presented the method of channel estimation on millimeter wave channel.[16] The IRS-assisted MIMO system is considered and channel estimation is performed by the two-stage

method and the IRS-supported transmission route is estimated by the approximate message transmission method.[17] In the study,[18] established the channel estimation based on sparse matrix factorization of the Internet of Things (IoT) system supported by the IRS. The latest research works,[19-21] successfully applied tensor models in many signal processing problems, especially for wireless communication systems. Semi-blind channel estimation methods for MIMO systems have also considered,[22,23] channel estimation methods for cooperative communication,[24,25] and more recently, estimation methods compressed channel in massive MIMO systems.[26,27]

In most of these works, signal processing is very efficient thanks to the uniqueness of tensor decomposition to exploit the multidimensional nature of transmitted/received signals and communication channels. The parallel factor (PARAFAC) structure of the tensor model is very convenient for the estimation problem of time varying multipath channel parameters by using pilot signal pattern and IRS phase shift signals in time domain.[28]

In this paper, the tensor model is used to extend the least squares channel estimation problem. Instead of solving the cascaded MIMO channel estimation problem, we propose the separate MIMO channel estimation problem between the base station transmitter to the IRS (BS-IRS) and between the IRS to the User Terminal (IRS-UT) by exploiting the PARAFAC structure. Accordingly, we set up two algorithms. The first algorithm is a closed-form solution based on the Khatri-Rao factorization (KRF) of the combination of BS-IRS and IRS-UT channels. The second algorithm performs an iterative Bilinear Alternating Least Squares (BALS). The first algorithm is a closed-form algebraic and less complex solution, the second one can operate under less restrictive conditions on the system parameters.

The contributions of this article are summarized as follows.

• Using tensor model to set up two LS channel estimation algorithms based on Khatri-Rao Factorization (KRF) and the Bilinear Alternating Least Squares (BALS).

• Consider the relationship between the IRS-assisted MIMO system parameters for the estimated matrix rank to make the problems feasible.

Notation and operator: Matrices are represented with boldface capital letters (**A**; **B**;…), and vectors are denoted by boldface lowercase letters (**a**; **b**;...). Tensors are symbolized by calligraphic letters. Transpose and pseudo-inverse of a matrix $\mathbf{A}$ are denoted as $\mathbf{A}^T$ and $\mathbf{A}^\dagger$. $\|\mathbf{A}\|_F$ denote the Frobenius norm of $\mathbf{A}$. The operator diag(**a**) forms a diagonal matrix out of its vector argument, while $*, \circ, \lozenge, \odot, \otimes$ denote the conjugate, outer product, Khatri Rao, Hadamard and Kronecker products, respectively. $\mathbf{I}_N$ denotes the $N \times N$ identity matrix. The operator vec(·) vectorizes an $I \times J$ matrix argument, while $\text{unvec}_{I\times J}(\cdot)$ does the opposite operation. Moreover, vecd(·) forms a vector out of the diagonal of its matrix argument. The n-mode product between a tensor $\Upsilon \in \mathbb{C}^{I\times J\ldots K}$ and a matrix $\mathbf{A} \in \mathbb{C}^{I\times R}$ is denoted $\Upsilon \times_n \mathbf{A}$, for $1 \le n \le N$. The operator $D_i(\mathbf{A})$ forms a diagonal matrix from the i-th row of its matrix argument $\mathbf{A}$. Moreover, $\mathbf{A}_i$ denotes the i-th row of the matrix $\mathbf{A}$.

2. SIGNAL MODEL AND SYSTEM

In this article review the MIMO communication systems assisted by an IRS. The transmitter side is a Base Station (BS) equipped with an array of M_B antennas and the receiver side is a User Terminal (UT) with M_U antennas. The IRS consists of L passive elements, capable of individually adjusting their reflectances (i.e. phase shift control). The system model is illustrated in Figure 1.

https://doi.org/10.52111/qnjs.2023.17507

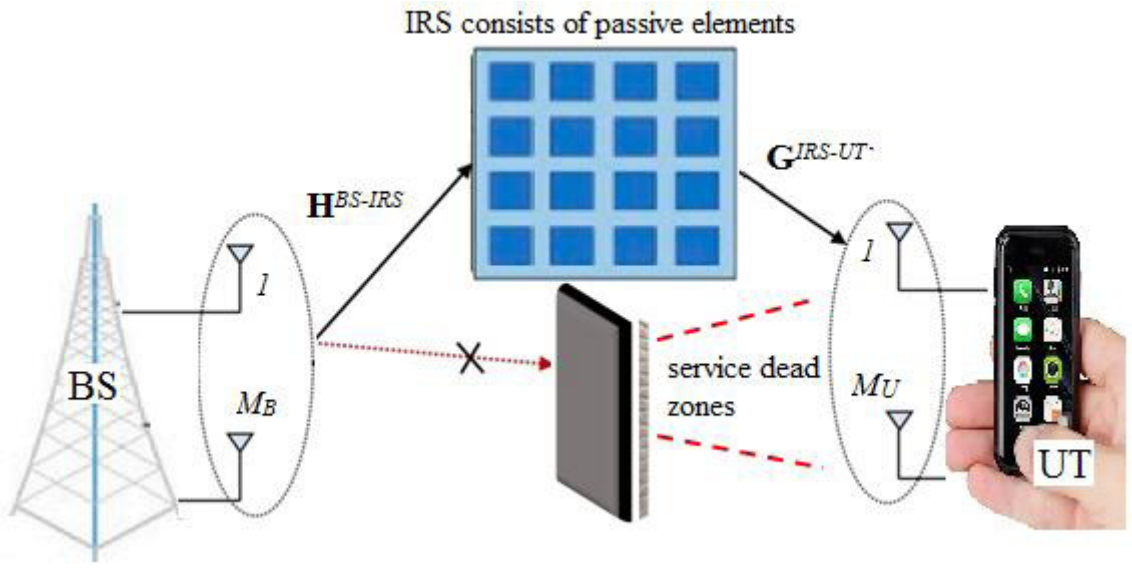

Figure 1. Model of the IRS-assisted MIMO system.

The signal at the device input can be represented by,[14,15]

$$\mathbf{y}[t] = \mathbf{G}^{IRS-UT}(\mathbf{s}[t] \odot \mathbf{H}^{BS-IRS}\mathbf{x}[t]) + \mathbf{n}[t], \quad 1 \le t \le T, \tag{1}$$

or in a different way,

$$\mathbf{y}[t] = \mathbf{G}^{IRS-UT}\text{diag}(\mathbf{s}[t])\mathbf{H}^{BS-IRS}\mathbf{x}[t]) + \mathbf{n}[t], \tag{2}$$

where, $\mathbf{x}[t] \in \mathbb{C}^{M_B \times 1}$ is a vector whose elements are transmitted pilot signals at time t, $\mathbf{s}[t]=\left[s_{1,t}e^{j\phi_1},...,s_{L,t}e^{j\phi_L}\right]^T \in \mathbb{C}^{L\times 1}$ is the vector that models the phase shifts and activation pattern of the IRS, where $\phi_n \in (0, 2\pi]$ is phase shift and $s_{n,t} \in \{0,1\}$ is the magnitude that controls the on-off state of the IRS elements at time t, respectively. $\mathbf{H}^{BS-IRS} \in \mathbb{C}^{L\times M_B}$ is the MIMO channel matrix from base station BS to IRS and $\mathbf{G}^{IRS-UT} \in \mathbb{C}^{M_U \times L}$ denote the MIMO channel between the IRS and the user terminal UT, and $\mathbf{n}[t] \in \mathbb{C}^{M_U \times 1}$ is the Additive White Gaussian Noise (AWGN) vector.

The training signal is modeled as shown in Figure 2. The training signal length T_s is divided into Q blocks, where each block is called a time slot of length T, i.e. $T_s = QT$. In expression (2), $\mathbf{y}[q,t] \triangleq y[(q-1)T+t]$ as the received signal at the t-th time slot of the q-th block, $t = 1,..., T$, $q = 1,..., Q$. Suppose, the time slot transmission, IRS adjusts its phase shifts as a function of time $t = 1,..., T$ and a block-fading channel, which means that the BS-IRS and IRS-UT channels are constant during T time slots.

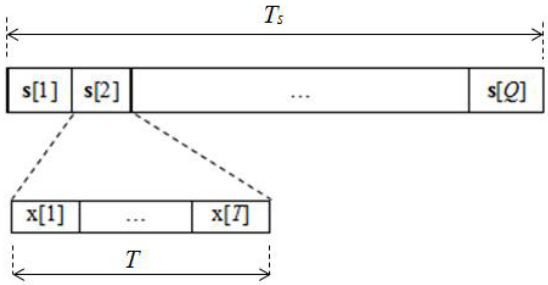

Figure 2. The time frame structure of the pilot signal pattern.

According to the signal frame structure in Figure 2, the IRS phase shift vector $\{\mathbf{s}[1],...,\mathbf{s}[Q]\}$ is constant during the T time slots of the q-th block and varies from block to block and the pilot signals $\{\mathbf{x}[1],...,\mathbf{x}[T]\}$ are repeated over the Q blocks. Mathematical representation in,[14]

$$\mathbf{s}[q,t] = \mathbf{s}[q], \ 1 \le t \le T \tag{3}$$

$$\mathbf{x}[q,t] = \mathbf{x}[q], \ 1 \le q \le Q \tag{4}$$

Accordingly, the signal in expression (2) is rewritten as

$$\mathbf{y}[q,t]=\mathbf{G}^{IRS-UT}\text{diag}(\mathbf{s}[q]\mathbf{H}^{BS-IRS}\mathbf{x}[t] + \mathbf{n}[q,t]. \tag{5}$$

All signals received in the time slot T of the q-th block, represented by the vector,

$\mathbf{Y}[q]=\left[\mathbf{y}[q,1]...\mathbf{y}[q,T]\right]\in\mathbf{C}^{M_U\times T}$ so we can perform,[14]

$$\mathbf{Y}[q]=\mathbf{G}^{IRS-UT}\text{diag}(\mathbf{s}[q])\mathbf{H}^{BS-IRS}\mathbf{X}^T+\mathbf{N}[q], \quad (6)$$

where, $\mathbf{X}\triangleq\left[\mathbf{x}[1],...,\mathbf{x}[T]\right]^T\in\mathbb{C}^{T\times M_B}$, and $\mathbf{N}\triangleq\left[\mathbf{n}[1],...,\mathbf{n}[T]\right]\in\mathbb{C}^{M_U\times T}$.

3. LEAST SQUARES (LS) CHANNEL ESTIMATION WITH TENSOR SIGNAL MODELING

Least Squares (LS) channel estimation is the most commonly used basic linear estimation method for channel estimation. LS channel estimation performs the minimum squared distance between the received signal and the transmitted signal.

To derive the LS estimate in the case in question, apply the property $\text{vec}(\mathbf{ABC})=\left(\mathbf{C}^T\lozenge\mathbf{A}\right)\text{vec}(\mathbf{B})$ and transform the expressions from (1) to (6), we have:

$$\begin{aligned}\mathbf{y}[q]&=\left\{\mathbf{X}(\mathbf{H}^{BS-IRS})^T\lozenge\mathbf{G}^{\text{IRS-UT}}\right\}\mathbf{s}_q\\&=\left(\mathbf{X}\otimes\mathbf{I}_{M_U}\right)\left\{(\mathbf{H}^{BS-IRS})^T\lozenge\mathbf{G}^{\text{IRS-UT}}\right\}\mathbf{s}[q]+\mathbf{n}[q],\end{aligned} \quad (7)$$

where,

$\mathbf{y}[q]\triangleq\text{vec}(\mathbf{Y}[q])\in\mathbb{C}^{M_UT}$,

$\mathbf{n}[q]\triangleq\text{vec}(\mathbf{N}[q])\in\mathbb{C}^{M_UT}$ and we have used property $(\mathbf{A}\otimes\mathbf{B})(\mathbf{C}\lozenge\mathbf{D})=(\mathbf{AC})\lozenge(\mathbf{BD})$.[28,29]

Defining $\mathbf{Y}\triangleq\left[\mathbf{y}[1]...\mathbf{y}[Q]\right]\in\mathbb{C}^{M_UT\times Q}$ and $\tilde{\mathbf{X}}\triangleq(\mathbf{X}\otimes\mathbf{I}_{M_U})\in\mathbb{C}^{TM_U\times M_BM_U}$, we have

$$\tilde{\mathbf{Y}}=\tilde{\mathbf{X}}\left\{(\mathbf{H}^{BS-IRS})^T\lozenge\mathbf{G}^{IRS-UT}\right\}\mathbf{S}^T+\mathbf{N}, \quad (8)$$

where, $\mathbf{S}\triangleq\left[\mathbf{s}[1],...,\mathbf{s}[Q]\right]^T\in\mathbb{C}^{Q\times L}$, and $\mathbf{N}\in\mathbb{C}^{M_UT\times Q}$ is the noise matrix set up in the same way as $\mathbf{Y}$. Finally, defined $\mathbf{y}\triangleq\text{vec}\left(\tilde{\mathbf{Y}}\right)\in\mathbb{C}^{M_UTQ}$, and apply the property $vec(\mathbf{ABC})=\left(\mathbf{C}^T\otimes\mathbf{A}\right)vec(\mathbf{B})$ to expression (8), we have

$$\mathbf{y}=\left(\mathbf{S}\otimes\tilde{\mathbf{X}}\right)\text{vec}\left\{(\mathbf{H}^{BS-IRS})^T\lozenge\mathbf{G}^{\text{IRS-UT}}\right\}+\mathbf{n} \quad (9)$$

or simply write in $\mathbf{y}=\mathbf{U}\boldsymbol{\theta}+\mathbf{n}$, (10)

where, $\mathbf{U}\triangleq\mathbf{S}\otimes\tilde{\mathbf{X}}\in\mathbb{C}^{QTM_U\times LM_BM_U}$, and $\boldsymbol{\theta}\triangleq\text{vec}\left\{(\mathbf{H}^{BS-IRS})^T\lozenge\mathbf{G}^{\text{IRS-UT}}\right\}\in\mathbb{C}^{M_BM_UL}$ is the composite channel parameter, combining the BS-IRS and IRS-UT channels. Estimating the LS channel applied to the composite channel in our case is the minimum of the problem,[6]

$$\hat{\boldsymbol{\theta}}=\arg\min_{\boldsymbol{\theta}}\left\|\mathbf{y}-\mathbf{U}\boldsymbol{\theta}\right\|^2, \quad (11)$$

the solution (11) results found $\boldsymbol{\theta}=\mathbf{U}^{\dagger}\mathbf{y}$. Applying the Kronecker product of $\mathbf{U}$, this solution can be simply rewritten $\boldsymbol{\theta}=(\mathbf{S}^{\dagger}\otimes\tilde{\mathbf{X}}^{\dagger})\mathbf{y}$.

In the conventional LS estimation problems just presented, the composite channel linear parameter vector $\boldsymbol{\theta}$ does not use the Katri-Rao structure. This is unfortunate, because the signal expression (6), or its equivalent (8) can be written as a parallel factor (PARAFAC) tensor model. The application of tensor model allows to improve the accuracy of channel estimation compared to traditional LS methods. This can compute a separate estimate for the $\mathbf{H}^{BS-IRS}$ and $\mathbf{G}^{IRS-UT}$ channels instead of the composite channel estimate $\boldsymbol{\theta}$.

To simplify the signal modeling by tensor operation, we first ignore the noise component in expression (6), leaving only the signal component, so we can rewrite as

$$\hat{\mathbf{P}}[q]=\mathbf{G}^{IRS-UT}\mathbf{D}_q(\mathbf{S})\mathbf{Z}^T,\ \mathbf{Z}\triangleq\mathbf{X}\left(\mathbf{H}^{BS-IRS}\right)^T\in\mathbb{C}^{T\times L}, \quad (12)$$

where, $\mathbf{D}_q(\mathbf{S})\triangleq\text{diag}(\mathbf{s}[q])$ denotes diagonal matrix of the q-th row of the IRS phase shift matrix $\mathbf{S}$ on its main diagonal. The matrix $\hat{\mathbf{P}}[q]$ can be viewed as the q-th front matrix slice of the 3-dimensional tensor $\overline{\Upsilon}\in\mathbb{C}^{M_U\times T\times Q}$; according to the PARAFAC decomposition. This operation is also the Canonical Polyadic Decomposition (CPD). Each (m, t, q)-th element of the received signal tensor, regardless of noise, is written in,[28-31]

$$\hat{p}_{m,t,q}=\sum_{n=1}^{L}g_{m,n}z_{t,n}s_{q,n}, \quad (13)$$

where, $g_{l,n}\triangleq[\mathbf{G}^{IRS-UT}]_{m,n}$, $z_{t,n}\triangleq[\mathbf{Z}]_{t,n}$, $s_{q,n}\triangleq[\mathbf{S}]_{q,n}$.

The abbreviation for PARAFAC decomposition (13) is written as $\overline{\Upsilon}=\left[\mathbf{G}^{IRS-UT},\mathbf{Z},\mathbf{S}\right]$. Using n-mode product notation, the PARAFAC decomposition

https://doi.org/10.52111/qnjs.2023.17507

of the zero-noise received signal tensor can be represented by,[28,29]

$$\bar{\Upsilon} = \Gamma_{3,L} \times_1 \mathbf{G}^{IRS-UT} \times_2 \mathbf{Z} \times_3 \mathbf{S}. \quad (14)$$

Exploiting the linear triple of the PARAFAC decomposition, we can expand the received signal tensor $\bar{\Upsilon}$ in the form of three matrices as follows,[28,29]

$$\hat{\mathbf{P}}_1 = \mathbf{G}^{IRS-UT}(\mathbf{S} \lozenge \mathbf{Z})^T \in \mathbb{C}^{M_U \times TQ}, \quad (15)$$

$$\hat{\mathbf{P}}_2 = \mathbf{Z}(\mathbf{S} \lozenge \mathbf{G}^{IRS-UT})^T \in \mathbb{C}^{M_U \times TQ}, \quad (16)$$

$$\hat{\mathbf{P}}_3 = \mathbf{S}(\mathbf{Z} \lozenge \mathbf{G}^{IRS-UT})^T \in \mathbb{C}^{Q \times M_U T}, \quad (17)$$

where, $\hat{\mathbf{P}}_1 \triangleq \left[\hat{\mathbf{P}}[1],...,\hat{\mathbf{P}}[K]\right]$, $\hat{\mathbf{P}}_2 \triangleq \left[\hat{\mathbf{P}}^T[1],...,\hat{\mathbf{P}}^T[Q]\right]$ $\hat{\mathbf{P}}_3 \triangleq \left[\text{vec}(\hat{\mathbf{P}}[1]),...,\text{vec}(\hat{\mathbf{P}}[Q])\right]^T$.

Next, the algebraic structure of the PARAFAC (13) model is exploited to establish two methods of channel estimation. The PARAFAC model is very usable thanks to its essential factor identification uniqueness property, which is derived from the concept of Kruskal rank (*k*-rank).

4. PROPOSAL TO EXTEND LS CHANNEL ESTIMATION UNDER TENSOR SIGNAL MODEL

In this section, we extend the estimating $\mathbf{H}^{BS-IRS}$ and và $\mathbf{G}^{IRS-UT}$ channel matrices from the Tensor signal modeling is presented as shown in (13). First, we define, $\Upsilon \triangleq \bar{\Upsilon} + \mathbb{N}$ as the noise-corrupted received signal tensor, where $\mathbb{N} \in \mathbb{C}^{M_U \times T \times Q}$ is the additive noise tensor. Similarly, $\mathbf{P}_i \triangleq \hat{\mathbf{P}}_i + \mathbf{N}_i$, $i = 1,2,3$ are the 1-mode, 2-mode, and 3-mode extended matrix noise versions respectively in the tensor expressions of the received signal (15-17), và $\mathbf{N}_{i=1,2,3}$ corresponds to the extended matrices of the noise tensor.

In this study, the pilot signal matrix $\mathbf{X}$ calculated using semi-unitary matrices satisfying $\mathbf{X}^H\mathbf{X} = T\mathbf{I}_{M_B}$, same for the phase shifts matrix IRS $\mathbf{S}$ is $\mathbf{S}^H\mathbf{S} = Q\mathbf{I}_L$. A best option for computing $\mathbf{X}$ and $\mathbf{S}$ matrices is to use truncated Discrete Fourier transform (DFT) matrices.

4.1. LS channel estimation based on Khatri-Rao Factorization

We can first rewrite the noise expansion matrix (17) as

$$\begin{aligned}\mathbf{P}_3 &= \mathbf{S}(\mathbf{Z} \lozenge \mathbf{G}^{IRS-UT})^T + \mathbf{N}_3 \\ &= \mathbf{S}\left[(\mathbf{H}^{BS-IRS})^T \lozenge \mathbf{G}^{IRS-UT}\right]^T \left[(\mathbf{H}^{BS-IRS})^T \lozenge \mathbf{G}^{IRS-UT})\right]^T + \mathbf{N}_3,\end{aligned} \quad (18)$$

in the transformations of the above expression, we used the property, $\mathbf{A} \otimes \mathbf{B}\ \ \mathbf{C} \lozenge \mathbf{D} = \mathbf{AC} \lozenge \mathbf{BD}$

Applying a bilinear filter on the time domain at the receiver by exploiting the knowledge of the IRS matrix and the pilot signal matrix, as follows

$$\mathbf{X}^\dagger \otimes \mathbf{I}_{M_U}\ \mathbf{P}_3^T\ \mathbf{S}^{T\ \dagger} = \mathbf{H}^{BS-IRS\ T} \lozenge \mathbf{G}^{IRS-UT} + \tilde{\mathbf{N}}_3 \triangleq \mathbf{\Omega}, \quad (19)$$

where, $\tilde{\mathbf{N}}_3 = \mathbf{X}^\dagger \otimes \mathbf{I}_{M_U}\ \mathbf{N}_3^T\ \mathbf{S}^{T\ \dagger}$ is the noise component after filtering. Note, $\mathbf{\Omega} \in \mathbb{C}^{M_B M_U \times L}$ is the Khatri-Rao structured noise version of the virtual MIMO channel in an IRS-assisted MIMO systems. Based on the semi-unitary structure of the $\mathbf{S}$ and $\mathbf{X}$ matrices, the correlation properties of the additive noise are not affected by the bilinear filter step.

From expression (19), we deduce the estimation of the $\mathbf{H}^{BS-IRS}$ and $\mathbf{G}^{IRS-UT}$ matrices by the Khatri-Rao least squares approximation problem,

$$\min_{\mathbf{H},\mathbf{G}} \left\| \mathbf{\Omega} - (\mathbf{H}^{BS-IRS})^T \lozenge \mathbf{G}^{IRS-UT} \right\|_F^2. \quad (20)$$

The efficiency of this problem is thanks to the application of the KRF (Khatri-Rao factorization) algorithm. Expression (20) can be understood as finding the $\mathbf{H}^{BS-IRS}$ and $\mathbf{G}^{IRS-UT}$ matrix estimators to minimize the set rank 1 matrix approximations, [28,32,33]

$$\hat{\mathbf{H}}^{BS-IRS}, \hat{\mathbf{G}}^{IRS-UT} = \arg\min_{\mathbf{h}_n,\ \mathbf{g}_n} \sum_{n=1}^{L} \left\| \tilde{\mathbf{\Omega}}_n - \mathbf{g}_n \mathbf{h}_n^T \right\|_F^2, \quad (21)$$

where,

$\tilde{\mathbf{\Omega}}_n \triangleq \text{unvec}_{M_U \times M_B}\ \mathbf{\omega}_n\ \in \mathbf{C}^{M_U \times M_B}$, $\mathbf{g}_n \in \mathbf{C}^{M_U \times 1}$, and

https://doi.org/10.52111/qnjs.2023.17507

$\mathbf{h}_n^T \in \mathbf{C}^{1\times M_B}$ are the n-th column of $\mathbf{G}^{IRS\text{-}UT}$ matrix, and n-th row of $\mathbf{H}^{BS\text{-}IRS}$ matrix, respectively. The estimates of $\mathbf{g}_n$ and $\mathbf{h}_n$ in (21) can be obtained from the left and right dominant singular vectors $\tilde{\mathbf{\Omega}}_n$, respectively, with $1 \le n \le L$, respectively. Thus, the estimation problem under consideration is transformed into L approximation submatrix problems of rank 1. Once we find $\hat{\mathbf{H}}^{BS-IRS}$ and $\hat{\mathbf{G}}^{IRS-UT}$ from (21), we can set up a composite channel $\boldsymbol{\theta}$.

4.2. BALS channel estimation

From the noise versions of the expansion matrix in expressions (15) and (16), we can derive an iterative solution based on the Bilinear Alternating Least Squares algorithm. This algorithm is a simplified version of the Trilinear Alternating Least Squares algorithm for estimating the factor matrices of the PARAFAC model.[34] In this case, since the matrix $\mathbf{S}$ is known at the receiver, the $\mathbf{G}^{IRS\text{-}UT}$ and $\mathbf{H}^{BS\text{-}IRS}$ matrices are estimated by the method of interleaving by optimizing in the iterative process of the following two cost functions,[34]

$$\hat{\mathbf{G}}^{IRS-UT} = \arg\min_{\mathbf{G}^{IRS-UT}} \left\| \mathbf{P}_1 - \mathbf{G}^{IRS-UT} \left[\mathbf{S} \lozenge \mathbf{X}(\mathbf{H}^{BS-IRS})^T \right]^T \right\|_F^2, \tag{22}$$

$$\hat{\mathbf{H}}^{BS-IRS} = \arg\min_{\mathbf{H}^{BS-IRS}} \left\| \mathbf{P}_2 - \mathbf{X}(\mathbf{H}^{BS-IRS})^T \left[\mathbf{S} \lozenge \ \mathbf{G}^{IRS-UT\ T} \right]^T \right\|_F^2, \tag{23}$$

the results of the solutions are:

$$\hat{\mathbf{G}}^{IRS-UT} = \mathbf{P}_1 \left[\left[\mathbf{S} \lozenge \mathbf{X} \ \mathbf{H}^{BS-IRS\ T} \right]^T \right]^{\dagger}, \tag{24}$$

$$\hat{\mathbf{H}}^{BS\text{-}IRS\ T} = \mathbf{X}^{\dagger}\mathbf{P}_2 \left[\ \mathbf{S} \lozenge \mathbf{G}^{IRS-UT\ T} \right]^{\dagger}, \tag{25}$$

The convergence is declared when $\left\| e_{(i)} - e_{(i-1)} \right\| \le \delta$, with $e_{(i)} = \left\| \Upsilon - \hat{\Upsilon}_{(i)} \right\|_F^2$ is the the the reconstruction erro calculated at the i-th iteration, δ a threshold parameter, and $\hat{\Upsilon}_{(i)} = \left[\hat{\mathbf{G}}^{IRS-UT}, \mathbf{X}\left(\hat{\mathbf{H}}^{BS-IRS}\right)_{(i)}^T, \hat{\mathbf{S}} \right]$ is the reconstructed PARAFAC model (c.f (6), (13)) from the estimated channel matrices $\hat{\mathbf{G}}_{(i)}^{IRS-UT}$ and $\hat{\mathbf{H}}_{(i)}^{BS-IRS}$ at the end of the i-th iteration.

If the matrices $\mathbf{X}$ and $\mathbf{S}$ have orthogonal columns (requires $Q \ge L$ and $T \ge M_U$ are required), the right pseudo-inverse in (24) and (25) can be repeated by matrix products. This results in a low complexity BALS algorithm with simple estimation steps.

The common feature of the two algorithms is that the cascaded channel estimation is achieved by separating the estimates of the two $\mathbf{G}^{IRS\text{-}UT}$ and $\mathbf{H}^{BS\text{-}IRS}$ channel matrices, which improves the performance compared to the direct estimation of the cascaded channel using the conventional least squares algorithm. By focusing on pilot-assisted channel estimation methods, we improve the algorithm in,[39] to have a more comprehensive formulation of IRS-assisted channel estimation methods. Based on the tensor model, thereby giving necessary notes useful for the design of training parameters.

4.3. Feasibility conditions of extended estimation algorithms

The KRF method with a bilinear filter step as in (19) requires an IRS phase shift matrix $\mathbf{S}$ and the pilot symbol matrix $\mathbf{X}$ have full column rank, subject to the following conditions:

$$Q \ge L \text{ and } T \ge M_B \tag{26}$$

As mentioned earlier, it is best to choose the $\mathbf{X}$ and $\mathbf{S}$ matrices as semi-unitary (or column-orthogonal) matrices. It is explained that instead of inverting the matrices in (19) we use semi-unitary single matrix products to simplify processing at the receiver. In addition, the correlation properties of the noise component after filtering in (19) are preserved.

The BALS method requires two Khatri-Rao products $\mathbf{\Lambda}_1 = \mathbf{S} \lozenge \mathbf{X} \ \mathbf{H}^{BS-IRS\ T} \in \mathbb{C}^{QT\times L}$ and $\mathbf{\Lambda}_2 = \mathbf{S} \lozenge \mathbf{G}^{IRS-UT} \in \mathbb{C}^{QM_U\times L}$ have full column rank, such that (24) and (25) admit unique solutions. This means that the conditions $QT \ge L$ and $QM_U \ge L$ must be satisfied. Combining these two inequalities results in $\min(QT, QM_U) \ge L$, or equivalently, $Q\min(T, M_U) \ge L$. Also notice that the condition $T \ge M_B$ in (23) is required,

https://doi.org/10.52111/qnjs.2023.17507

since $\mathbf{X}$ must have the full column rank to be left inverse. Therefore, the following conditions are necessary

$$Q\min(T,\ M_U) \geq L \text{ và } T \geq M_B. \quad (27)$$

Comparing conditions (26) and (27), we can see that the BALS estimation method has less constraints on the minimum number of time blocks Q for the training channel than the KRF method. In the special case $M_U = 1$ (MISO or SISO systems, respectively), the inequalities (26) and (27) equal signs occur, meaning that BALS and KRF are subject to the same training requirements. Obviously BALS algorithm has advantages over KRF when applied in MIMO system, because BALS can work with $Q < L$, while KRF requires $Q \geq L$. Note that, if $Q = 1$, KRF estimation method is equivalent to conventional LS estimator. However, in this case we cannot solve/separate the estimation problem of two channel matrices through solving problem (20). On the other hand, the KRF algorithm has lower computational complexity than BALS, which will be presented later in the results section and discussed in the following section.

In addition, it should be noted that (27) is a necessary but not guaranteed condition for the uniqueness of BALS estimates. The sufficient condition can be derived from the rank characteristics of the matrices $\mathbf{S} \lozenge \mathbf{X}\ \mathbf{H}^{BS-IRS\ T} \in \mathbb{C}^{QT \times L}$ and $\mathbf{S} \lozenge \mathbf{G}^{IRS-UT} \in \mathbb{C}^{QM_U \times L}$.

To ensure the uniqueness of the channel estimates in solving problems (22) and (23) for matrices in Khatri-Rao form, applying the lemmas in,[35,36] the result is

$$\text{rank}(\mathbf{S}) + \text{rank}\left[\mathbf{X}\left(\mathbf{H}^{BS-IRS}\right)^T\right] \geq L+1 \quad (28)$$

$$\text{rank}(\mathbf{S}) + \text{rank}(\mathbf{G}^{IRS-UT}) \geq L+1 \quad (29)$$

We are considering the channel training parameters, specifically calculating such that the IRS phase shift matrix $\mathbf{S}$ and the pilot symbols matrix $\mathbf{X}$ have full rank. These conditions are useful for system design when using the BALS estimation method.

4.3.1. Full rank of channel matrix $\boldsymbol{H}^{BS-IRS}$ and $\boldsymbol{G}^{IRS-UT}$

Assuming that both $\mathbf{H}^{BS-IRS}$ and $\mathbf{G}^{IRS-UT}$ channel matrices have full rank (in case of Rayleigh fading channel), the condition (28)-(29) can be rewritten as

$$\min(Q, L) + \min(M_B, L) \geq L + 1 \quad (30)$$

$$\min(Q, L) + \min(M_U, L) \geq L + 1 \quad (31)$$

We can distinguish two cases as follows.

• $L \geq T \geq M_B$ and $L \geq M_U$: In this case, the base station BS and user equipment UT have small antenna array size, the number of BS and UT antennas is smaller than the number of IRS elements. Condition (28)-(29) becomes

$$M_B + \min(Q, L) \geq L + 1 \quad (32)$$

$$M_U + \min(Q, L) \geq L + 1 \quad (33)$$

• $T \geq M_B \geq L$: In this case, the base station BS is assumed to be equipped with a large antenna array. The minimum number of BS antennas is equal to the number of IRS elements (massive MIMO system setup). Since condition (28) is always satisfied for all values of Q, the uniqueness of the channel estimate depends only on (29), that is

$$\min(Q, L) + \min(M_U, L) \geq L + 1 \quad (34)$$

Conditions (32) and (33) establish a trade-off between the time dimension (the number of IRS training blocks Q) and the two spatial dimensions (the number of transmitting antennas M_B and the number of receiving antennas M_U) for the case channel restore. For example, if $Q < L$, this condition implies $M_B + Q \geq L + 1$ and $M_U + Q \geq L + 1$, which is equivalent to $\min(M_B + Q, M_U + Q) \geq L + 1$. That is, the number of transmitting (or receiving) antennas can be reduced while ensuring that the unique characteristic of the BALS channel estimation method is compensated by increasing the number of time blocks Q.

4.3.2. The $\boldsymbol{H}^{BS-IRS}$ and $\boldsymbol{G}^{IRS-UT}$ channel matrices lack rank

In millimeter wave MIMO systems, a large number of transmit/receive antennas coupled

https://doi.org/10.52111/qnjs.2023.17507

with a poorly scattered propagation medium can result in low-rank $\mathbf{H}^{BS\text{-}IRS}$ and $\mathbf{G}^{IRS\text{-}UT}$ channel matrices. Assume that the signal propagating between the BS base station and the IRS via C_1 clusters, while the signal propagating between the IRS and the user terminal UT through the C_2 cluster. Also, suppose that each cluster contributes a ray of complex amplitude and forms the angle of incidence or angle of departure. We can represent the $\mathbf{H}^{BS\text{-}IRS}$ and $\mathbf{G}^{IRS\text{-}UT}$ channel matrices as follows,[37]

$$\mathbf{H}^{BS-IRS} = \mathbf{A}_{IRS}\text{diag}(\boldsymbol{\alpha})\mathbf{A}_{BS}^{H}, \quad (35)$$

$$\mathbf{G}^{IRS-UT} = \mathbf{B}_{UT}\text{diag}(\boldsymbol{\beta})\mathbf{B}_{IRS}^{H}, \quad (36)$$

where, $\mathbf{A}_{\text{BS}} \in \mathbb{C}^{M_B \times C_1}$, $\mathbf{A}_{\text{IRS}} \in \mathbb{C}^{L \times C_1}$, $\mathbf{B}_{UT} \in \mathbb{C}^{M_U \times C_2}$, $\mathbf{B}_{\text{IRS}} \in \mathbb{C}^{L \times C_2}$ are array response matrices, and the vectors $\boldsymbol{\alpha}$, $\boldsymbol{\beta}$ are the complex amplitude coefficients of the BS-IRS and IRS-UT channels. In case of lack of rank, then rank($\mathbf{H}^{BS\text{-}IRS}$) = C_1 and rank($\mathbf{G}^{IRS\text{-}UT}$) = C_2, with $C_1 \leq \min(M_B, L)$ and $C_2 \leq \min(M_U, L)$.

Considering condition (26), the lack of rank of the channel matrix does not affect the solution of the channel estimation problem for the KRF algorithm. However, for the case of BALS estimation, since the uniqueness of the LS estimate of the $\mathbf{G}^{IRS\text{-}UT}$ and $\mathbf{H}^{BS\text{-}IRS}$ matrices depends on the rank of these matrices, as shown in conditions (28) and (29). For the BALS estimate, we can derive the following useful results.

• Case $T \geq M_B$: Conditions (28) and (29) become

$$\min(Q, L) + \text{C}_1 \geq L + 1 \quad (37)$$

$$\min(Q, L) + \text{C}_2 \geq L + 1 \quad (38)$$

The following scenarios are possible. If $Q \geq L$, we conclude that these conditions are always satisfied, for every ranks of the channel matrices. If $Q < L$, these conditions become $Q + \text{C}_1 \geq L + 1$ and $Q + \text{C}_2 \geq L + 1$, which is useful for choosing a block number Q that ensures the uniqueness of the channel estimates in the case lack of rank.

• Case $Q \geq L$: In this case, conditions (28) and (29) are always satisfied, for all ranks of the $\mathbf{G}^{IRS\text{-}UT}$ and $\mathbf{H}^{BS\text{-}IRS}$ matrices.

5. SIMULATION RESULTS AND DISCUSSION

In this section, some simulation results are presented to evaluate the performance of the channel estimation methods in this article and compare them with similar methods. The channel estimates are evaluated in terms of the Normalized Mean Square Error NMSE given by,[6]

$$\text{NMSE}\left(\hat{\mathbf{H}}^{BS-IRS}\right) = \frac{1}{C}\sum_{r=1}^{C}\frac{\left\|\left(\mathbf{H}^{BS-IRS}\right)^{(l)} - \left(\hat{\mathbf{H}}^{BS-IRS}\right)^{(l)}\right\|_F^2}{\left\|\left(\mathbf{H}^{BS-IRS}\right)^{(l)}\right\|_F^2}, \quad (39)$$

where, $\left(\hat{\mathbf{H}}^{BS-IRS}\right)^{(l)}$ is the estimated BS-IRS channel at the l-th run, C represents the number of Monte Carlo runs. Similar definitions apply to the $\left(\hat{\mathbf{G}}^{IRS-UT}\right)^{(l)}$ channel estimation.

The SNR(dB) ratio is defined as

$$\text{SNR(dB)} = 10\log_{10}\left(\frac{\left\|\bar{\Upsilon}\right\|_F^2}{\left\|\mathbb{N}\right\|_F^2}\right), \quad (40)$$

where, $\bar{\Upsilon}$ is the generated noiseless received signal tensor corresponding to the expression (13), $\mathbb{N}$ is the additive noise tensor.

In the simulation calculations, assuming the elements of the channel matrices $\mathbf{H}^{BS\text{-}IRS}$ and $\mathbf{G}^{IRS\text{-}UT}$ are independent and identically distributed (i.i.d) zero-mean circularly-symmetric complex Gaussian random variables. Note that the estimated channel matrix elements $\hat{\mathbf{H}}^{BS\text{-}IRS}$ and $\hat{\mathbf{G}}^{IRS\text{-}UT}$ in expression (21) of the KRF algorithm found using the SVD (Singular Value Decomposition) tensor operation $t-\text{SVD}(\tilde{\boldsymbol{\Omega}}_n)$.[32,33] In order to facilitate the evaluation of the quality of the algorithms, we choose the same system parameters as the reference articles, depending on each case.

Figure 3 depicts the NMSE performance curves in terms of SNR (dB) for the KRF and BALS algorithms. This is the result of system parameters $T = 4$, $M_B = 4$, $M_U = 2$, $Q = 50$ and the

https://doi.org/10.52111/qnjs.2023.17507

number of IRS elements with different values L = 10, 50. In this article, the BALS estimation calculations, we choose $e = 10^{-5}$. Although the number of iterations of the BALS algorithm is natural, only a few iterations can be converged (usually less than 10 iterations) thanks to the information that the IRS matrix **S** remains constant across the iterations.

Observing the results of Figure 3, we see that both algorithms give the desired performance. With the same number of IRS elements L, the estimated performance of the two algorithms KPF and BALS is similar. In terms of complexity, the KRF algorithm has a lower complexity but more restrictive requirements for the training parameter Q. While the iterative BALS method, although computationally more complex, can operate under more flexible choices of system parameters and with lower training costs. The system parameter constraints we discussed in section 4.3. On the other hand, the NMSE performance decreases as the number of IRS elements increases L, which is the expected result since the number of channel coefficients in the matries $\mathbf{G}^{IRS\text{-}UT}$ và $\mathbf{H}^{BS\text{-}IRS}$ to be estimated also increases with L. This means that it is possible to increase the system estimation performance while reducing the structural complexity of the IRS.

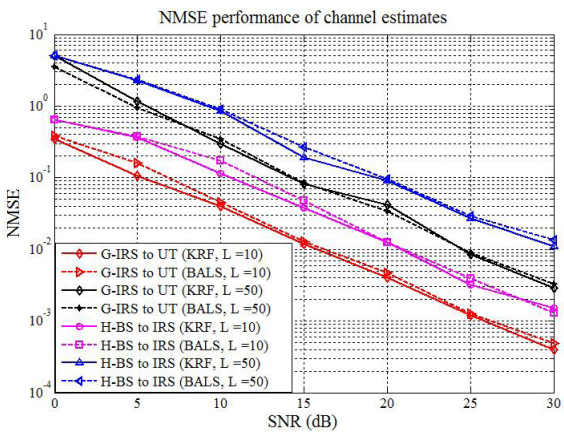

Figure 3. NMSE performance of channel estimates $\hat{\mathbf{H}}^{BS\text{-}IRS}$ và $\hat{\mathbf{G}}^{IRS\text{-}UT}$.

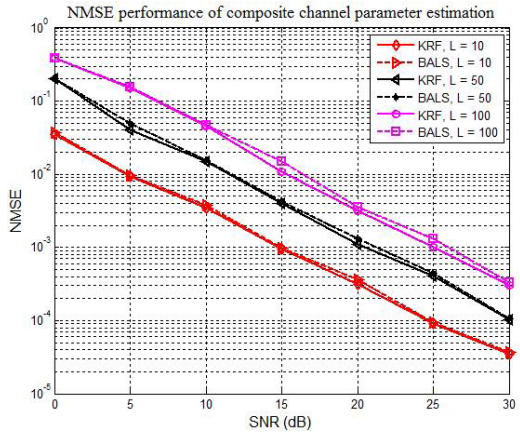

Figure 4. NMSE performance of composite channel parameter estimation $\hat{\boldsymbol{\theta}}$.

Figure 4 is the result of calculating the NMSE performance of estimating the composite parameter vector $\boldsymbol{\theta}$ according to the parameters Q = 100, T = 4, M_B = 3, M_U = 20, and L has the values 10, 50, 100. This result is consistent with the results of Figure 3, the estimated efficiency decreases as the number of IRS elements L increases. Another method to overcome the performance degradation presented in,[40] is to divide the IRS elements into groups of activation/deactivation in a time-domain sequential manner. However, this method will increase the total training time by a factor proportional to the number of element groups.

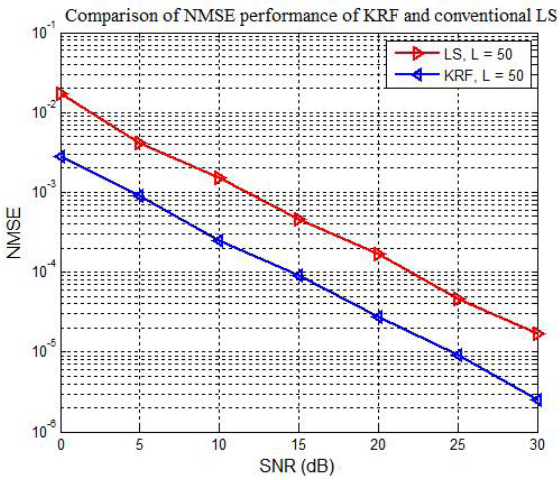

Figure 5. Comparison of NMSE performance of KRF estimator and conventional LS estimator.

In Figure 5, we compare the estimation results of the KRF algorithm with the conventional LS method. In this result, we choose

$Q=L=50$, $T=M_B=20$, $M_U=8$. The conventional LS method plotted on the graph is to estimate the composite channel parameter vector, ignoring the Khatri-Rao structure that is attenuated during the signal model vectorization. In contrast, the KRF algorithm in this paper exploits the Khatri-Rao channel structure and establishes from channel estimation matrices the $\hat{\mathbf{H}}^{BS\text{-}IRS}$ và $\hat{\mathbf{G}}^{IRS\text{-}UT}$.

In Figure 6 is the NMSE performance estimate of the lacking rank $\hat{\mathbf{H}}^{BS\text{-}IRS}$ và $\hat{\mathbf{G}}^{IRS\text{-}UT}$ channel matrices. In this result, the channel matrices are created according to the model (35)-(36), the channel parameters are selected, $Q = L = 64$, $M_U = 4$ and $T = M_B = 4$; 20, where $C_1 = C_2 = 1$. For comparison, we use the NMSE results of the LS channel estimation method proposed in.[38]

Observing the results of Figure 6, we see that the KRF algorithm has superior performance compared to the conventional LS algorithm. The gain in terms of SNR is about 7dB. This result is explained by the fact that KRF effectively exploits the Khatri-Rao structure present in the equivalence channel model.

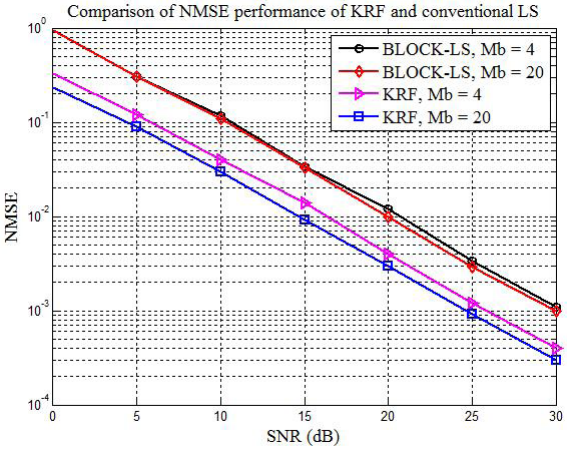

Figure 6. NMSE estimation results of composite channel parameter vector $\hat{\boldsymbol{\theta}}$ in the case of matrices $\hat{\mathbf{H}}^{BS\text{-}IRS}$ và $\hat{\mathbf{G}}^{IRS\text{-}UT}$ lacking rank.

Note that the KRF algorithm solves the problem by reshaping $M_B M_U \times L$ Khatri-Rao channels as L IRS subchannels of size $M_B \times M_U$, increasing noise rejection by rank-1 approximation steps. As M_B and M_U increase in large numbers (corresponding to a masive MIMO systems), the larger the noise spread over the noise subspace and, therefore, the higher the level of noise rejection achieved. This is a special feature of the KRF channel estimation algorithm that the conventional LS channel estimation algorithm cannot exploit.

In study,[38] the pilot signal time frame was the same as in this study, consisting of dividing the total training time into Q blocks and an IRS phase shift pattern that varied from block to block. In,[38] the LS estimation method is used by dividing the training signal frame T into blocks, referred to as the "block-LS" method for short. In this result, we compare the KRF estimation algorithm in this paper with the block-LS estimation method in.[38] We can see that the KRF estimation algorithm outperforms the block-LS estimation method in.[38] The authors in,[38] showed that the performance of the block-LS method was not affected as the number of M_B transmitting antennas and the pilot sequence length T increased. This is in contrast to the KRF method which provides more accurate channel estimation as the antenna arrays are larger. Specifically, the SNR gain of the KRF algorithm compared to the block-LS method is nearly 4.5 dB for $M_B = 4$ and increased to 5.5 dB for $M_B = 20$. This can be explained as follows. For the KRF algorithm, through exploiting the Khatri-Rao structure of the cascaded channel, the level of noise cancellation is higher when the number of M_B transmitting antennas or M_U receiving antennas is increased. However, this advantage comes at the expense of increased computational complexity, as well as increased length of pilot sequences.

6. CONCLUSION AND DEVELOPMENT DIRECTION

In this paper, we have extended the LS channel estimation algorithm for MIMO information system assisted by IRS based on tensor model. The KRF and BALS channel estimation algorithms are established by efficiently

https://doi.org/10.52111/qnjs.2023.17507

exploiting the tensor structure of the received signal. Both algorithms perform separate estimation of the transmission channels between the BS to the IRS and from the IRS to the UT with the passive elements of the IRS. The closed-form KRF algorithm has lower complexity but more restrictive requirements for training parameter Q. While BALS iterative method, although computationally more complex, can operate on more flexible choices for training parameter Q with lower training cost. In this article, we also consider the relationship between the system parameters to ensure the uniqueness of the channel estimates. These constraints are useful when designing system channel estimates. Some simulation and discussion calculation results, we have demonstrated the superior performance of KRF and BALS compared with the conventional LS estimator, ignoring the Khatri-Rao structure of the combined channel matrix. In the proposal of this paper, in section 4.3, we give useful recommendations for the selection of system parameters to ensure the uniqueness of channel estimation.

The KRF and BALS channel estimation algorithms mentioned in this paper can improve the performance by exploiting the knowledge of the rank of the estimation matrices, or, using compression sensing methods to take advantage of the sparse representation of the $\mathbf{H}^{BS\text{-}IRS}$ and $\mathbf{G}^{IRS\text{-}UT}$ channel matrices. This could be the next research direction of interest.

Acknowledgments

The authors would like to thank the editor(s) and anonymous reviewers for their constructive comments and suggestions that have helped to improve the present paper.

REFERENCES

1. M. D. Renzo, H. Haas, A. Ghrayeb, S. Sugiura, and L. Hanzo. Spatial modulation for generalized MIMO: Challenges, opportunities, and implementation, *Proceedings of the IEEE*, **2014**, *102*(1), 56103.
2. F. Boccardi, R. W. Heath, A. Lozano, T. L. Marzetta, and P. Popovski. Five disruptive technology directions for 5G, *IEEE Communications Magazine*, **2014**, *52*(2), 74-80.
3. P. Yang, M. Di Renzo, Y. Xiao, S. Li, and L. Hanzo. Design guidelines for spatial modulation, *IEEE Communications Surveys & Tutorials*, **2015**, *17*(1), 6-26.
4. S. Rangan, T. S. Rappaport, and E. Erkip. MillimeterWave cellular wireless networks: Potentials and challenges, *Proceedings of the IEEE*, **2014**, *102*(3), 366-385.
5. S. Gong, X. Lu, D. T. Hoang, D. Niyato, L. Shu, D. I. Kim, and Y.-C. Liang. Toward smart wireless communications via intelligent reflecting surfaces: A contemporary survey, *IEEE Communications Surveys & Tutorials*, **2020**, *22*(4), 2283-2314.
6. C. Pan, G. Zhou, K. Zhi, S. Hong, T. Wu, Y. Pan, H. Ren, M. D. Renzo, A. L. Swindlehurst, R. Zhang, A. Y. Zhang. An overview of signal processing techniques for RIS/IRS-aided wireless systems, *IEEE Journal of Selected Topics Signal Processing*, **2022**, *16*(5), 883-917.
7. B. Zheng, C. You, W. Mei, and R. Zhang. A survey on channel estimation and practical passive beamforming design for intelligent reflecting surface aided wireless communications, *IEEE Communications Surveys & Tutorials*, **2022**, *24*(2), 1035-1071.
8. Q. Wu and R. Zhang. Towards smart and reconfigurable environment: Intelligent reflecting surface aided wireless network, *IEEE Communications Magazine*, **2020**, *58*(1), 106-112.
9. Q. Wu and R. Zhang. Beamforming optimization for wireless network aided by intelligent reflecting surface with discrete phase shifts, *IEEE Transactions on Communications*, **2020**, *68*(3), 1838-1851.
10. Y. Song, M. R. A. Khandaker, F. Tariq, and K.-K. Wong. *Truly intelligent reflecting surface-aided secure communication using deep learning,* IEEE 93rd Vehicular Technology Conference, April 2021.

11. L. Dong and H.-M. Wang, Secure MIMO transmission via intelligent reflecting surface, *IEEE Wireless Communication Letters*, **2020**, *9*(6), 787-790.

12. A. Taha, M. Alrabeiah, and A. Alkhateeb. Enabling large intelligent surfaces with compressive sensing and deep learning, *IEEE Access,* **2021**, *9*, 1-19.

13. T. L. Jensen and E. D. Carvalho. *An optimal channel estimation scheme for intelligent reflecting surfaces based on a minimum variance unbiased estimator*, ICASSP 2020-2020 IEEE International Conference on Acoustics, Speech and Signal Processing (ICASSP), 2020.

14. Z. He and X. Yuan. Cascaded channel estimation for large intelligent metasurface assisted massive MIMO, *IEEE Wireless Communication Letters*, **2020**, *9*(2), 210-214.

15. B. Ning, Z. Chen, W. Chen, and Y. Du. *Channel estimation and transmission for intelligent reflecting surface assisted THz communications*, ICC 2020-2020 IEEE International Conference on Communications (ICC), 2020.

16. Y. Han, W. Tang, X. Li, M. Matthaiou and S. Jin. CSI acquisition in RIS-assisted mobile communication systems, *Informatics and Commuter Journal,* **2023**, 1-15.

17. J. Mirza and B. Ali. Channel estimation method and phase shift design for reconfigurable intelligent surface assisted MIMO networks, *IEEE Transactions on Cognitive Communications and Networking,* **2021**, *7*(2), 441-451.

18. S. Xia and Y. Shi. *Intelligent reflecting surface for massive device connectivity: Joint activity detection and channel estimation*, ICASSP 2020-2020 IEEE International Conference on Acoustics, Speech and Signal Processing (ICASSP), 2020.

19. Y. Zniyed, R. Boyer, A. L. de Almeida, and G. Favier. Tensor train representation of MIMO channels using the JIRAFE method, *Signal Processing,* **2020**, *171*.

20. Y. Zniyed, R. Boyer, A. L. F. Almeida, and G. Favier. High-order tensor estimation via trains of coupled third-order CP and Tucker decompositions, *Linear Algebra and Its Applications,* **2020**, *588*, 304-307.

21. Y. Zniyed, R. Boyer, A. L. Almeida, and G. Favier. A TT-based hierarchical framework for decomposing high-order tensors, *SIAM Journal on Scientific Computing*, **2020**, *42*(2), A822-A848.

22. A. L. F. de Almeida, X. Luciani, A. Stegeman, and P. Comon. Confac decomposition approach to blind identification of underdetermined mixtures based on generating function derivatives, *IEEE Transactions on Signal Processing*, **2012**, *60*(11), 5698-5713.

23. A. L. de Almeida, G. Favier, and J. C. Mota. A. L. de Almeida, G. Favier, and J. C. Mota. Space time spreading multiplexing for MIMO wireless communication systems using the PARATUCK-2 tensor model, *Signal Processing*, **2009**, *89*(11), 2103-2116.

24. W. Freitas, G. Favier, and A. L. F. de Almeida. Generalized Khatri-Rao and Kronecker space-time coding for MIMO relay systems with closed-form semi-blind receivers, *Signal Processing*, **2018**, *151*, 19-31.

25. B. Sokal, A. L. de Almeida, and M. Haardt. Semi-blind receivers for MIMO multi-relaying systems via rank-one tensor approximations, *Signal Processing*, **2020**, *166*.

26. D. C. Araujo, A. L. F. de Almeida, J. P. C. L. Da Costa, and R. T. de Sousa. Tensor-based channel estimation for massive MIMO-OFDM systems, *IEEE Access*, **2019**, *7*, 42133-42147.

27. P. R. B. Gomes, A. L. F. de Almeida, J. P. C. L. da Costa, and R. T. de Sousa Jr. Joint DL and UL channel estimation for millimeter wave MIMO systems using tensor modeling, *Wireless Communications and Mobile Computing*, **2019**, 1-13.

28. V. D. Nguyen, K. A. Meraim, N. L. Trung. *Parallelizable PARAFAC decomposition of 3-way tensors*, Proceedings of European Signal Processing Conference (EUSIPCO) IEEE, 2015.

29. T. G. Kolda and B. W. Bader. Tensor decompositions and applications, *SIAM Review*, **2009**, *51*(3), 455-500.

https://doi.org/10.52111/qnjs.2023.17507

30. P. Comon, X. Luciani, and A. L. F. de Almeida. Tensor decompositions, alternating least squares and other tales, *Journal of Chemometrics*, **2009**, *23*(7), 393-405.

31. A. L. F. de Almeida, G. Favier, J. P. C. L. da Costa, and J. C. M. Mota. Overview of tensor decompositions with applications to communications, *Signals and Images: Advances and Results in Speech, Estimation, Compression, Recognition, Filtering, and Processing*, **2016**, *12*, 325-356.

32. A. Y. Kibangou and G. Favier. *Non-iterative solution for PARAFAC with a toeplitz matrix factor*, 2009 17th European Signal Processing Conference, 2009.

33. F. Roemer and M. Haardt. Tensor-based channel estimation and iterative refinements for two-way relaying with multiple antennas and spatial reuse, *IEEE Transactions on Signal Process*, **2010**, *58*(11), 5720-5735.

34. R. Bro. *Multi-way analysis in the food industry: Models, algorithms & applications,* Ph.D. dissertation, University of Amsterdam, 1998.

35. A. Stegeman and N. D. Sidiropoulos. On kruskal's uniqueness condition for the PARAFAC decomposition, *Linear Algebra and Its Applications*, **2007**, *420*(2), 540-552.

36. N. D. Sidiropoulos and R. Bro. On the uniqueness of multilinear decomposition of n-way arrays, *Journal of Chemometrics*, **2000**, *14*(3), 229-239.

37. R. W. Heath, N. Gonzalez-Prelcic, S. Rangan, W. Roh, and A. M. Sayeed. An overview of signal processing techniques for millimeter wave MIMO systems, *IEEE Journal of Selected Topics in Signal Processing*, **2016**, *10*(3), 436-453.

38. B. Li, Z. Zhang, Z. Hu. Channel estimation for reconfigurable intelligent surface-assisted multiuser mmWave MIMO system in the presence of array blockage, *Transactions on Emerging Telecommunications Technologies*, **2021**, *32*.

39. G. T. de Araujo and A. L. F. de Almeida. *PARAFAC-based channel estimation for intelligent reflective surface assisted MIMO system,* IEEE 11th Sensor Array and Multichannel Signal Processing Workshop (SAM), 2020, 1-5.

40. C. You, B. Zheng, and R. Zhang. *Intelligent reflecting surface with discrete phase shifts: Channel estimation and passive beamforming,* ICC 2020-2020 IEEE International Conference on Communications (ICC), 2020.